

An experimental investigation on melting and solidification behavior of phase change material in cylindrical latent heat storage units with minichannel

Eda Feyza Akyurek, Mehmet Yoladi*

High Technology Application and Research Center, Erzurum Technical University, Erzurum 25050, Turkey

ARTICLE INFO

Keywords:

Energy storage
Heat transfer
Minichannel
Phase change materials

ABSTRACT

The latent heat storage using phase change materials (PCM) has relative advantages compared to other thermal energy storage methods, according to numerous studies in the literature. The design of the heat exchanger are very important for performances of latent heat storage systems. Although there are studies using PCM in different design heat exchangers in recent years, they are quite limited. In this study, a design different from the literature has been used to create an alternative to latent energy storage (LHS) systems by passing different diameter minichannel through a cylindrical enclosure. The thermal effect of the PCM on both the charge and discharge process have been studied at different inlet temperatures of the HTF. Moreover, different flow rates of HTF and different minichannel diameters have been studied only for the charge process. According to the experimental results, as the inlet temperature has been raised from 60°C to 65°C, 70°C, 75°C, 80°C, start of the melting time has decreased by 51.22%, 62.99%, 64.46%, 73.28%, respectively. As the minichannel diameter has been decreased from 1.9mm to 1.5mm and from 1.5mm to 1.21mm, the liquid fraction has decreased by 10.6 and 50.5%, respectively, for 75°C HTF inlet temperature conditions. Additionally, the results has showed that the effect of HTF flow rate on thermal energy storage (TES) can be negligible. It was concluded that the optimal shell-tube radius ratio could be up to about 25 in the LHTES systems studied. It is a very important result for engineering systems using PCM for energy storage in heat exchangers.

1. Introduction

The increase in energy demand, environmental pollution, and energy crisis concerns during in the last years, have deemed it necessary to store the maximum amount of energy produced and benefit from the stored energy to the maximum extent. One of the most practical and ways of protecting the available energy and improving its usage is thermal energy storage (TES). Using TES systems for the discrepancy between the energy demand and supply is an appropriate method. It is advantageous to use phase change materials (PCMs) that are used in latent heat storage units as heat storage mediums as they have high energy storage density and isothermal phase transition (small temperature fluctuation) [1]. Latent TES systems that use PCMs can store 5-14 times more energy compared to other storage materials used at the same volume [2]. In recent years, many studies have been conducted on using PCMs in latent heat storage units for the practices such as heating and cooling buildings [3,4]; solar energy [5,6]; hot water [7] and; electronic cooling [8,9]. As

a result of the advances energy storage can be achieved at microscale. The decrease in size requires an increase in the yields of storing heat energy and using the stored energy. The effects of the energy storage properties in macro-scale systems on smaller-scale systems must be studied. When TES systems are used with PCMs in heat exchangers, the heat can be transferred to the PCM with a heat transfer fluid (HTF) and can be stored for future use. The selection of the PCMs for such applications depends on the working temperature of the system. When the studies in literature were examined, it was observed that melted salts were used to recover waste heat in high working temperatures, while paraffin was used to recover waste heat in low temperatures used for heating homes. Cunha and Eames examined different PCMs at specific temperatures and determined that it was appropriate to use salt hydrates and organic compounds for temperatures below 100°C, inorganic salt hydrates for those between 130°C and 1250°C and potassium and sodium for temperatures of 170°C [10]. Latent heat storage depends on the performance of the systems, the thermophysical properties of the PCM

* Corresponding author.

E-mail address: mehmet.yoladi@erzurum.edu.tr (M. Yoladi).

<https://doi.org/10.1016/j.est.2021.102938>

Received 21 January 2021; Received in revised form 7 July 2021; Accepted 8 July 2021

Available online 28 July 2021

2352-152X/© 2021 Elsevier Ltd. All rights reserved.

Table 1
Summary of the studies in the literature.

References	Study Type	PCM	Phase Change Process	Direction of the Heat Exchanger	Parameters	Important Results
[18]	Numerical	Eutectic mixture of lauric and stearic acids	Melting-Solidification	Vertical	Lauric and stearic acids mixture ratio, HTF inlet temperature, mass flow rate	<ul style="list-style-type: none"> • The mixture encapsulated in the annulus of two concentric pipes had good thermal and heat transfer properties during the melting and solidification processes. • The melting process was shortened with the increase in the inlet temperature and mass flow rate. • Heat transfer rate decreased with decreasing inlet temperature and mass flow
[19]	Experimental	Paraffin wax	Melting-Solidification	Horizontal	Effects of HTF working conditions (HTF inlet temperature, mass flow rate), exterior pipe diameter, pipe length	<ul style="list-style-type: none"> • An increase in the inlet temperature of the HTF decreased the melting process. • In order the decreased the energy consumption, lower values of mass flow rate for the HTF are advised. • The charge period decreased to 68% according to the diameter. • Flow rate did not have a significant effect on storage. • The HTF temperature showed significant effect on the charge process. • The highest productivity of heat exchanger was achieved when the ratio of the inner diameter to the outer diameter was 4. • The increase in the HTF inlet temperature decreased the solidification mass ratio and activity, while it increased the NTU value. • PMC storage inclination angle has an important effect on PCM temperature distribution, PCM melting time. • With the usage of fins, the melting-solidification times were shortened by at least 14%. • With the usage of composite PCM materials, this time could be shortened by at least 20%. • While the HTF type affects the solidification time by at least 10% on the fin surface, its effect was not observed on the finless surface. • Higher HTF (water) inlet temperature, mass flow rate and fin height ensured a higher PCM heat charge rate and shorter total charging time. • The melting times of PCM1, PCM2 and PCM3 were found to decrease with the increase in the HTF inlet temperature. • The decrease in melting time was the highest in PCM1 and lowest in PCM3. • The downward movement of the inner tube decreased the melting time. • The increase in the HTF inlet temperature accelerated the melting time, while the increase of the mass flow rate had no effect.
[15]	Experimental	Paraffin wax	Melting-Solidification	Vertical	Inlet temperature, Mass Flow Rate	
[20]	Experimental	Not specified	Melting	Vertical	Shell and Tube Diameter, HTF flow rate and temperature	
[21]	Numerical	n-Eicosane	Melting	Vertical	Ratio of inner diameter to outer diameter, HTF inlet temperature	
[22]	Numerical-Experimental	Paraffin wax	Melting	Vertical-Horizontal	Inclination positions	
[23]	Numerical	Pure inorganic salt composite of inorganic salt/EG	Melting-Solidification	Horizontal	Fins, PCM types, HTF types	
[24]	Numerical	Not specified	Melting	Horizontal	HTF inlet temperature, mass flow rate and conductive fin height	
[25]	Experimental	$K_2CO_3(51)$ - $49Na_2CO_3$ (PCM1), $Li_2CO_3(20)$ - $60Na_2CO_3$ - $20K_2CO_3$ (PCM2), $Li_2CO_3(32)$ - $35K_2CO_3$ - $33Na_2CO_3$ (PCM3)	Melting	Horizontal	HTF inlet temperature, PCM type, body tube length	
[26]	Numerical	RT50	Melting	Horizontal	Downward movement of inner tube, HTF inlet temperature, mass flow rate	

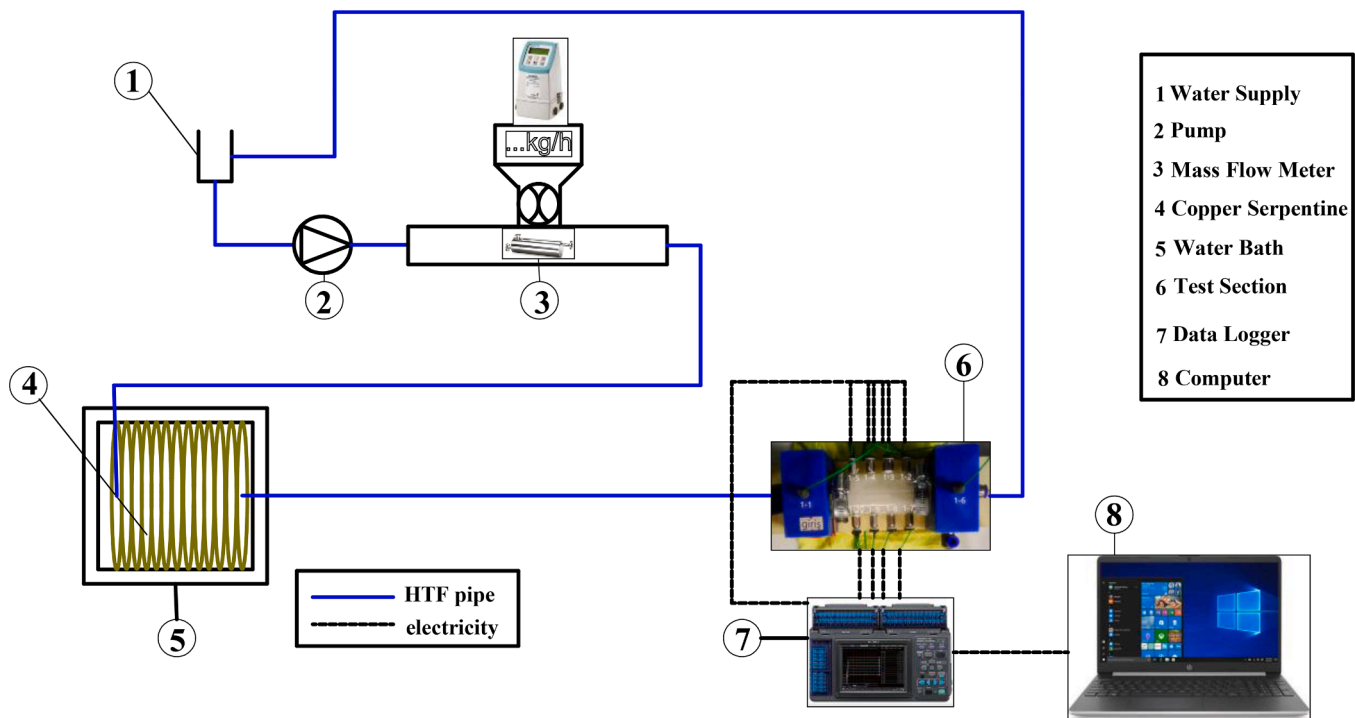


Fig. 1. Schematic diagram of the experimental setup.

and the design of the heat exchanger [11]. Heat exchange occurs within the PCM in two ways: conduction and convection. During the heat charging process, the heat transfer within the solid PCM only occurs through conduction, however when the PCM starts melting the heat transfer occurs between solid and fluid PCM through natural convection [12]. Joybari et al. investigated simultaneous charging and discharging of latent heat thermal energy storage numerically in a triplex tube heat exchanger. They used RT-31 as PCM and cooling fluids. The effect of natural convection on storage or charging was investigated. The effect of natural convection was found to be very small using the ε -NTU method. However, in this study, it was determined that the effect of natural convection was significant. It was stated that the upward melted PCM motion had a great effect on the process. No simultaneous charge/discharge dominance was determined. The best results were achieved with the conditions of interior adiabatic/exterior cooler and interior cooler/exterior heater [13].

There are many designs and applications regarding the usage of PCMs in heat exchangers. These applications give ideas about the parameters that should be applied to experimental setup. Heat exchangers should be designed to ensure faster charging and discharging by providing a higher effective heat transfer area. Cylindrical PCM enclosures are categorized into three types: the pipe model (HTF is in the cylinder), the cylinder model (HTF is out of the cylinder) and the shell and tube model (includes a lot of parallel tubes). Due to the advantages of easy design creation and minimum heat loss, approximately 70% of the researched TES systems consist of the shell and tube model [14].

Akgün et al., investigated the storage performance of the melting/solidification effect by using paraffin as PCM in the shell and tube heat exchanger. The main experimental parameters were the inlet temperature of the HTF and Reynolds number. They determined that increasing inlet temperature caused a decrease in the total melting time and the significance of Reynolds number was low [15]. In a TES system with a cylindrical enclosure, 0.204 kg n-eicosane was used PCM, 57°C HTF was passed through and melting was completed after 50 minutes. Some empty space was left in the upper section of enclosure for melting and solidification [16]. Kibria et al. computationally and experimentally investigated the heat transfer between PCM and HTF with different sizes

and working conditions of the shell and tube system in their studies. They found that the HTF inlet temperature had a significant effect on the PCM liquid fraction, while the mass flow rate had a small effect on the PCM liquid fraction. In addition, they determined that as the pipe diameter increased, the melting time decreased and HTF temperature difference increased [17]. Some of the studies performed about heat exchangers with PCM are given in Table 1.

There are new and more complex studies to improve heat transfer using PCM in heat exchangers. For example, Yang et al. examined the melting behavior of paraffin at different inclination angles in their work. Paraffin was embedded in open cell metal foams. In the study, it was concluded that the angle of inclination had a significant effect on the formation and development of natural convection during the melting of paraffin. It has been stated that the angle of inclination affects the solid-liquid interface propagation and heat transfer rate [27]. Qu et al., had developed a two-dimensional temporary model for a commercial square lithium ion battery using paraffin saturated in metallic copper foam. The estimated battery surface temperature was consistent with experimental data for the foam-paraffin composite during 1°C and 3°C discharge processes. Thus, the model has been verified in this study [28]. Ren et al. inserted woven metal fibers with high thermal conductivity into the phase change material to improve the heat transfer rate in their work. The corresponding energy storage process has been investigated in the latent heat storage unit, based on lattice Boltzmann modeling through numerical reconstruction of fiber morphology. According to results, it has been stated that woven metal fibers with optimum porosity should be used to balance the heat transfer capability and energy storage capacity of the woven metal fiber-phase change material composite [29]. Jiang and Qu used a sandwich cooling structure consisting of a battery, phase change material, and heat pipe in their study. It has been proved in the study that the collective thermal model could solve the coupling heat transfer in the cooling structure of the PCM and the heat pipe [30]. Ren et al., studied the thermal management of electronic devices using a pin-fin cascade microencapsulated phase change material (MEPCM) - expanded graphite (EG) composite-filled heat sink. 3D enthalpy-based lattice Boltzmann modeling has been used. It has been stated that a pin-fin array with a mid-fin number and fin thickness was beneficial to



Fig. 2. Actual photograph of the experimental setup.

balance for the MEPCM's increased heat transfer capacity and reduced latent heat. Thus, optimum thermal performance has been achieved [31]. Ren et al., designed novel stacked 2D metal fibers, inserting them into the microencapsulated phase change material (MEPCM) to improve the thermal performance of the heat sink. Thermal performance of heat sink assembly filled with MEPCM-metal fiber composite based on the numerically reconstructed metal fibers has been investigated. In the study, it was stated that for an intermittent heat sink, MEPCM stacked 2D metal fiber composite with a high anisotropic rating has a more obvious advantage in its thermal management [32].

As a result of the studies conducted, it can be said that there are different heat exchanger designs that can benefit from bidirectional heat transfer between HTF and PCM. PCM is usually used in shell and tube model heat exchangers and the amount of PCM and design of heat exchanger depends on the heat to be applied. One of the main problems regarding design with PCM concept is reducing the thermal resistance for both melting and solidification process. In order to reduce thermal resistance, methods that increase heat conductivity must be applied. The aim of present study was to observe and analyze how PCM react to phase characteristics by designing a new energy storage system for the melting (usually) and solidification processes of PCM. Thus, the effect of a novel system and unworked parameters on energy storage will respond to TES systems in various fields. Unlike the other studies in the literature, this study included a test area where HTF was passed through channels with very small minichannel diameters. The ratio of cylindrical outer enclosure's diameter to the minichannel diameter was 25. This study was carried out experimentally. The melting / solidification states of RT-50 as PCM were examined horizontally. The effects of parameters such as HTF inlet-outlet temperature, mini-channel diameter, mass flow rate on the thermal energy storage of PCM were investigated by a series of experiments. In this study, results indicated that the optimal shell to tube radius ratio should be less than approximately 5 in the studied LHTES systems [20]. Thus, in a design to be made in the field of engineering; the effect of many parameters such as mass flow rate and inlet temperature on the unworked the diameter ratio will contribute to the literature.

2. Experimental setup and LHTS test section

2.1. Experimental setup

The schematic demonstration of the system created in this study is given in Fig. 1, while photograph of the system is presented in Fig. 2. RT-50 paraffin, which had a melting range of approximately 45-51°C, was used as PCM for energy storing. When the PCM melts, thermal energy is stored (charge) and when it solidifies again (discharge), the energy it has stored is released. Until the melting process starts, the heat transfer occurs through conduction and after the melting process, it goes on with natural convection [33]. In Figs. 1 and 2 feedwater passed through a flowmeter by means of a pump and mass flow rate of the fluid was fixed to desired level. Then, the feedwater that was passed through a copper serpentine that came into contact with hot and cold water in a waterbath reached the test area after being heated up (charged) and cooled down (discharge). When hot water passed through the minichannel in the test area, the PCM (RT-50), which was located between the outer surface of minichannel and the inner surface of the plexiglass, melts (charge). On the other hand, the liquid PCM solidified (discharge) when cold water passed through. Location temperature values that changed in the test area, were taken with the help of a data logger. The record measurement data showed the instantaneous temperature values of the thermocouples in the test area. Its working principle works by converting electric current to temperature value. Hioki LR8402-20 brand data logger was used. In this study, the TES performance of the PCM, which was located between the outer surface of minichannel heat exchanger through which the HTF passes and the inner surface of the plexiglass enclosure was experimentally investigated by applying different parameters to the HTF.

2.2. LHTS test section

The test zone (plexiglass) was fixed with two polyethylene blocks in blue color. Canals were opened from the middle point of the blocks in order to pass the minichannelled tubes through. In addition, 9 cm cylindrical plexiglass was placed between the blocks to protect the PCM. Thus, thanks to the blocks, the connection between the minichannel and the fluid passing through the water bath will be provided. It will also

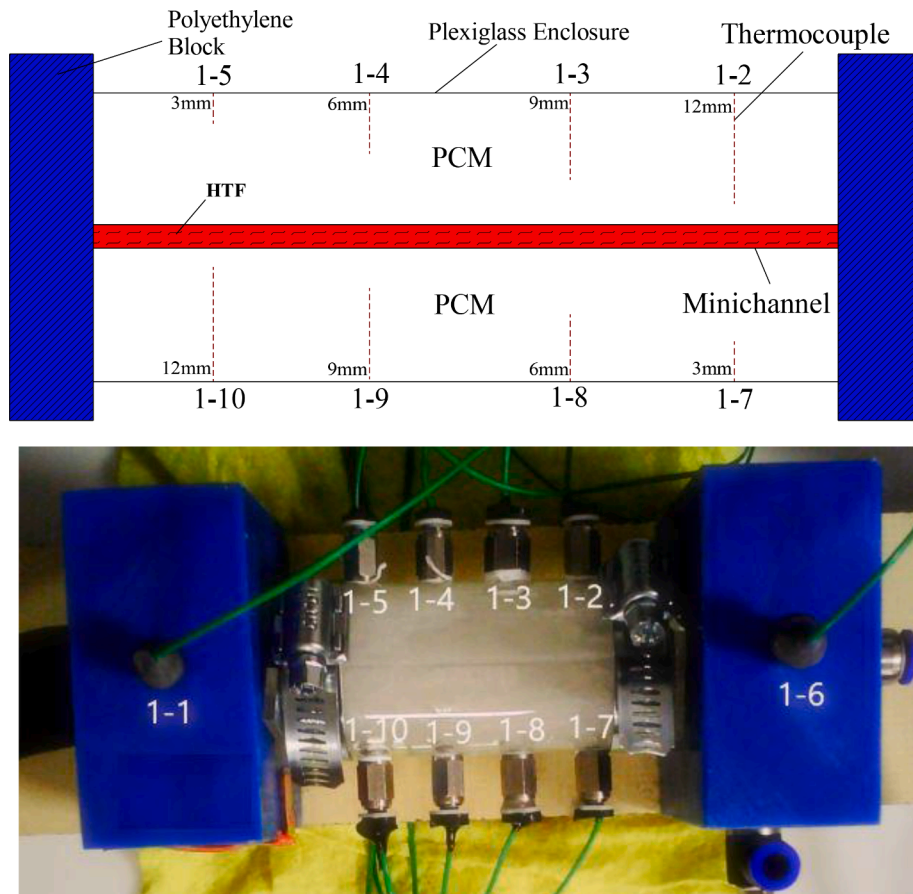


Fig. 3. Dimensions and photograph of the LHTS test section without insulation.

Table 2
Axial and radial positions of the thermocouples.

Thermocouple	Radial position (m)	Axial position (m)
1-2	0.012	0.072
1-3	0.009	0.054
1-4	0.006	0.036
1-5	0.003	0.018
1-7	0.003	0.072
1-8	0.006	0.054
1-9	0.009	0.036
1-10	0.012	0.018

prevent PCM leakage, which melts by squeezing the plexiglass. Then, the RT-50 PCM was filled between the inner surface of the plexiglass cylinder and the outer surface of the minichannel. Due to the 12.5% volume change of the PCM during the solid-fluid phase change, some space was left in the fluid state. The reason for this was to reduce the pressure

Table 3
Thermophysical properties of the PCM [35].

Properties	RT-50 (Phase Change Material)
Melting Area	45-51 [°C]
Congeeing Area	51-46 [°C]
Heat Storage Capacity	160 [kJ/kg]
Specific Heat Capacity	2 [kJ/kg.K]
Density Solid (at 15°C)	0.88 [kg/l]
Density Liquid (at 80°C)	0.76 [kg/l]
Heat Conductivity	0.2 [W/(m.K)]
Volume Expansion	% 12.5
Flash Point	>200 [°C]
Max. Operation Temperature	70 [°C]

applied to the wall in case of solidification resulting from the volume expansion. In Fig. 3, the thermocouples were 12mm, 9mm, 6mm and 3mm deep (B section) in the direction of the inlet to the outlet of the HTF and 12mm, 9mm, 6mm and 3mm deep (T section) in the direction of the outlet to inlet. They were placed diagonally in this way to examine the thermal effect of the HTF inlet and outlet in the same radial distance on a short channel length and to show the temperature change depending on the heat transfer progressing gradually in the radial direction and melting process. Fig. 3 shows the thermocouple connections and the test area. The diameter of the outer plexiglass enclosure was 36mm and three different diameters namely 1.21mm, 1.5mm and 1.9mm were used in the minichannel that was worked on.

Heat was transferred from the hot water passing through the mini-channel to the solid PCM by conduction. In addition, heat was transferred from the liquid PCM to the cold water passing through the minichannel by convection. Accordingly, melting (charge) or solidification (discharge) occurred. In addition, the constant matter in the system was expressed as the state of being completely liquid or solid on plane where the thermocouples were placed. The locations where thermocouples are placed, are given in Table 2.

2.3. Selection and properties of the PCM

In the selection of the PCM, parameters such as thermodynamic, kinematical, chemical, physical and economic properties were taken into consideration. Thermodynamically, the melting temperature must be operated in the low vapor pressure and desired melting temperature range to reduce the problems that restrict the melting in the reaction state [34]. It is kinematically important to avoid high reaction rates. By doing so, heat can be homogeneously absorbed from the system storage unit. The sudden decrease of the thermal resistance prevents the gradual

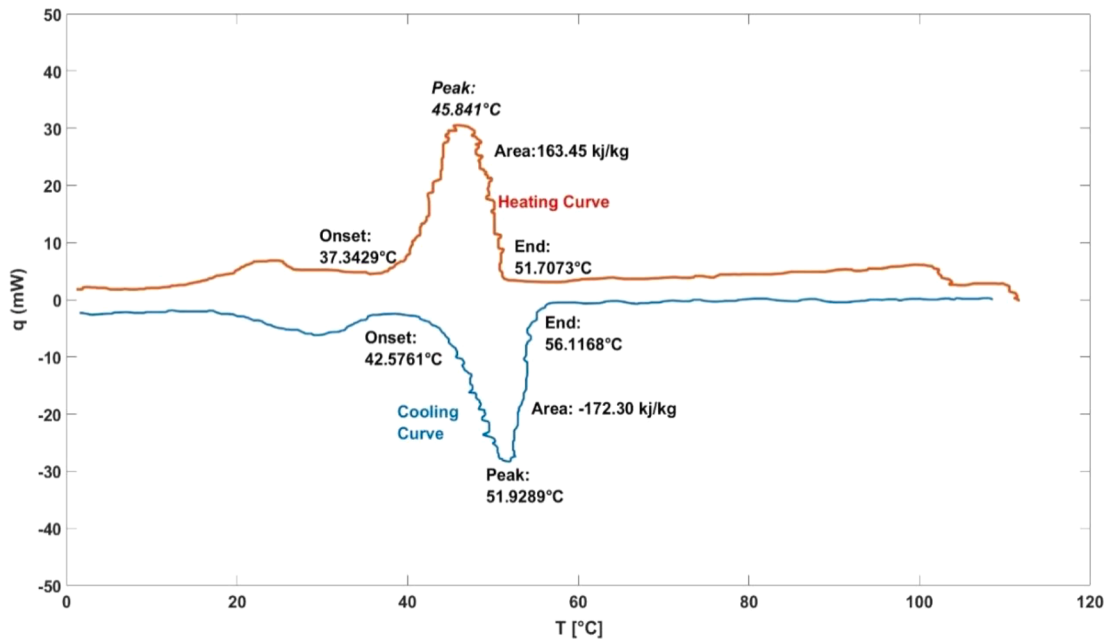


Fig. 4. Differential scanning calorimetry analysis curve of the PCM.

resistance transition and this ensures that the melting is not homogeneous. Materials that are low-cost and easily accessible should be selected. Care should be taken to avoid chemical degradation after successive phase cycles. Physically, during thermal storage the volume expansion should be kept at a minimum in order not to damage the system.

In this study, RT-50 brand paraffin was used as the PCM. The thermophysical properties of the PCM are shown in Table 3.

Differential Scanning Calorimetry (DSC) measures the absorbed or released energy amount of the PCM while it is being heated, cooled or kept at a constant temperature. Thus, the change in the amount of energy that occurs as a result of the heat transfer in the PCM and the reference used in the device is shown depending on temperature and time. In addition, with this method the heat transfer amount during the phase change in the PCM can be determined. DSC analysis can be considered as the PCM identity. When Table 3 and Fig. 4 are compared, a coherency between the thermophysical properties table and DSC analysis can be observed.

2.4. Uncertainty analysis

In this study, for the experimental errors the uncertainty theme applied by McClintock and Kline in 1953 was used. According to this method:

- R : The size measured
- $x_1, x_2, x_3, \dots, x_n$: The factors that affect the measuring result
- $w_1, w_2, w_3, \dots, w_n$: The error rate of the independent variable

Total error rate W_R :

$$W_R = \left[\left(\frac{\partial R}{\partial x_1} w_1 \right)^2 + \left(\frac{\partial R}{\partial x_2} w_2 \right)^2 + \left(\frac{\partial R}{\partial x_3} w_3 \right)^2 + \dots + \left(\frac{\partial R}{\partial x_n} w_n \right)^2 \right]^{1/2}$$

or

$$\frac{W_R}{R} = \left[\left(\frac{W_{x_1}}{x_1} \right)^2 + \left(\frac{W_{x_2}}{x_2} \right)^2 + \left(\frac{W_{x_3}}{x_3} \right)^2 + \dots + \left(\frac{W_{x_n}}{x_n} \right)^2 \right]^{1/2}$$

Table 4

Technical specifications and sensitivity of the measuring devices.

Materials	Technical Specifications	Sensitivity
Thermocouple	K type; Measuring range (-40°C and 375°C)	±1.5%
Flow Meter	Measuring range (0 / 250kg/h)	±0.1%
Pump	Measuring range (85.7ml/min - 2571.4ml/min)	±1%
Water Bath	Measuring range (-40°C and 100°C)	±0.1%
Data Logger	60 channel capacity	±0.1%

In uncertainty analyses it is sufficient to determine the variable that causes the biggest error.

The uncertainties of the most important parameters in the system, namely temperature and flow rate were calculated using the sensitivity values given in Table 4. As a result, the uncertainty value of the temperature measured in the experiment was calculated as ±1.5066, while the uncertainty value of the mass flow rate was calculated as ±1.00498. Heat transfer cumulative effect of uncertainties of temperature and flow rate was ±1.8110.

3. Experimental results and discussion

In this study, water was passed through a minichannel heat exchanger as HTF and the thermal behavior of RT-50 paraffin used as PCM was observed during the charging and discharging processes. The PCM was located between the inner tube and plexiglass outer tube. By passing the water through the inner channel (minichannel) at a constant temperature, the energy of the PCM during charging was changed. As the PCM melted, it stored energy as heat during the charge process. During discharge process, cold water at constant temperature was passed through the minichannel tube, causing the PCM to solidify and release its stored energy.

The experiments were carried out in accordance with the objectives given below.

- Effects of six different inlet temperatures (55, 60, 65, 70, 75, 80°C) on energy storage of PCM (charge) were investigated at 10 kg/h constant mass flow rate and 1.5mm inner channel diameter during 120 minute experiment period.

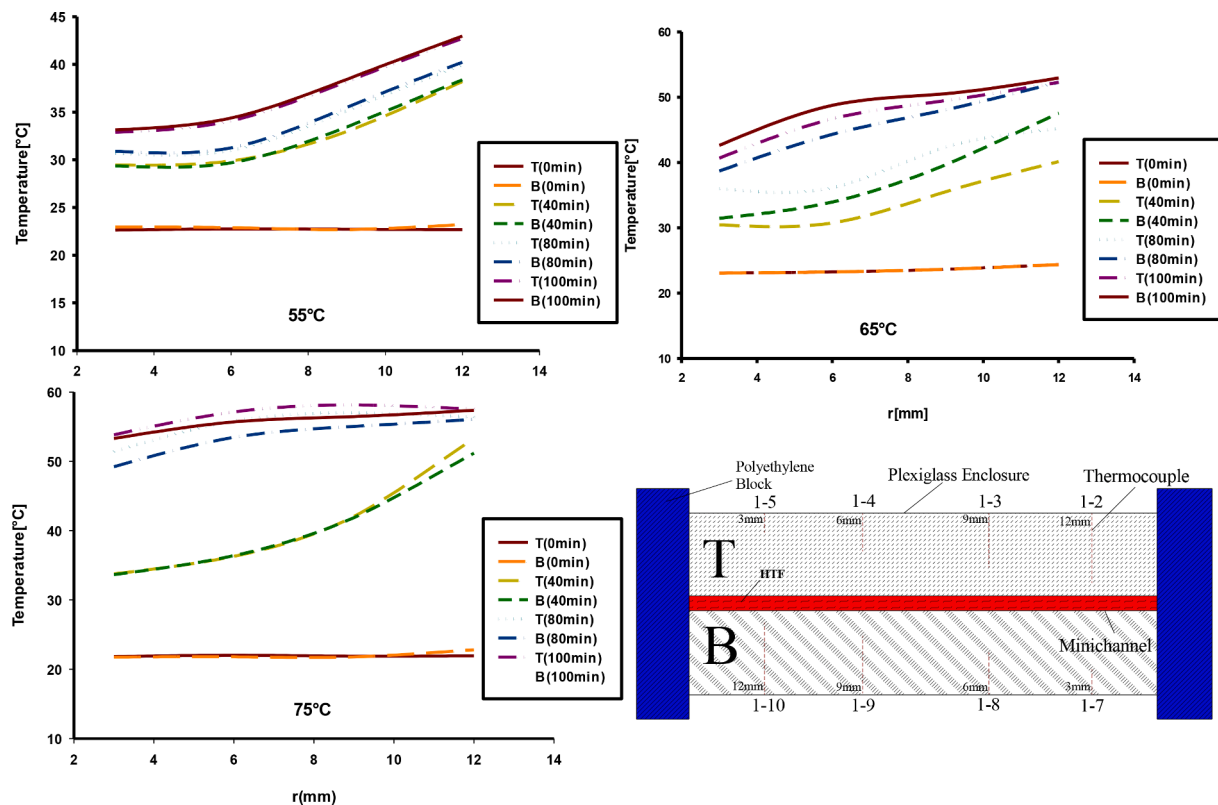


Fig. 5. Effect on radial distances of HTF inlet and outlet temperature differences during melting.

- Effects of three different HTF flow rates (4, 7 and 10 kg/h) on the energy storage of PCM (charge) were investigated at 1.5mm constant minichannel inner diameter and 75°C constant temperature.
- Effects of three different minichannel diameters (1.21mm, 1.5mm, 1.9mm) on the energy storage (charge) of PCM were investigated at 75°C constant temperature and 10kg/h constant flow rate.
- Finally, the effects of three different inlet temperatures (8°C, 15°C and 23°C) of HTF on releasing the energy stored by the PCM (discharge) were examined at 1.5mm constant minichannel inner diameter, and 10kg/h constant flow rate.

3.1. The effect of HTF's minichannel inlet and outlet on PCM during melting

The temperature effects of the HTF inlet and outlet on the radial direction were studied. Radial distance is defined as the distance from the minichannel through which the HTF flows to the outer surface of the plexiglass enclosure. The test area was divided into two different areas, namely T and B. The effect of the HTF inlet and outlet points to the test zone on the energy storage of the PCM can be interpreted according to the change in the temperature of the same location (e.g. points 1-2 and 1-10 at a depth of 12mm) in Fig. 5.

As the hot HTF that passed through the minichannel transferred heat to the PCM, the temperature of the PCM decreased as it approached the outer tube from the inner tube. Therefore, the temperature of the HTF towards the minichannel outlet is decreasing. Temperature change of the same radial distance is given in Fig. 5. As can be seen more clearly from Fig. 3, T and B sections are in the same axial plane. As expected, the maximum temperatures were observed in the locations that were close distance of 12mm distance away from the minichannel through which the HTF flowed. The farther away from the minichannel, heat transfer decreases and lower temperatures are achieved. For example points 1-9 and 1-3 at the same radial distance (9mm) has low temperature

difference (approximately 40-41°C) between the two points at 40th minute. Likewise, the temperature difference between 1-10/1-2(12mm), 1-4/1-8 (6mm) and 1-5/1-7(3mm) is also low at any given time. Therefore, the temperature of the locations that were of the same radial distance when lined up from the inlet to the outlet or from the outlet to the inlet were negligible. However, how the reaction will be in a longer test area must be studied.

3.2. The effect of the HTF inlet temperature on energy storage (charge)

The effect of different HTF inlet temperatures on melting during a constant mass flow rate was examined. As the inlet temperature increases, the phase change accelerates. As the melting temperature of the PCM was 50°C, the inlet temperature of the HTF started from 55°C and as the maximum working temperature of PCM was 70°C, the final inlet temperature of HTF was studied at 80°C.

With each inlet temperature, the temperature change in the radial direction decreased as it moved towards the outer enclosure. As can be seen from Fig. 6, among the location temperatures, the temperature was at the maximum usually at the 1-10 location closest to the HTF inlet area and the minichannel. Melting did not occur with the inlet temperature of 55°C. Thus, the heat transfer only occurred through conduction except for the flow in the minichannel. With the inlet temperature of 60°C, a liquid film formed on the upper section of the cylindrical plexiglass; thus, although very little, some melting occurred. In a broad sense, as the heat transfer occurred through convection, the temperature distribution in the thermocouple did not change. With the temperature of 65°C, although very little, some melting occurred. Some differences in location temperature values were observed after 2000 sec, due to the melting effects and natural convection. With this inlet temperature, complete melting in the radial direction was not achieved. At an inlet temperature of 70°C, as the PCM approaches the melting temperature, the location temperatures increases above one another. This was explained by the fact that the solid PCM melts the heat transfer natural convection

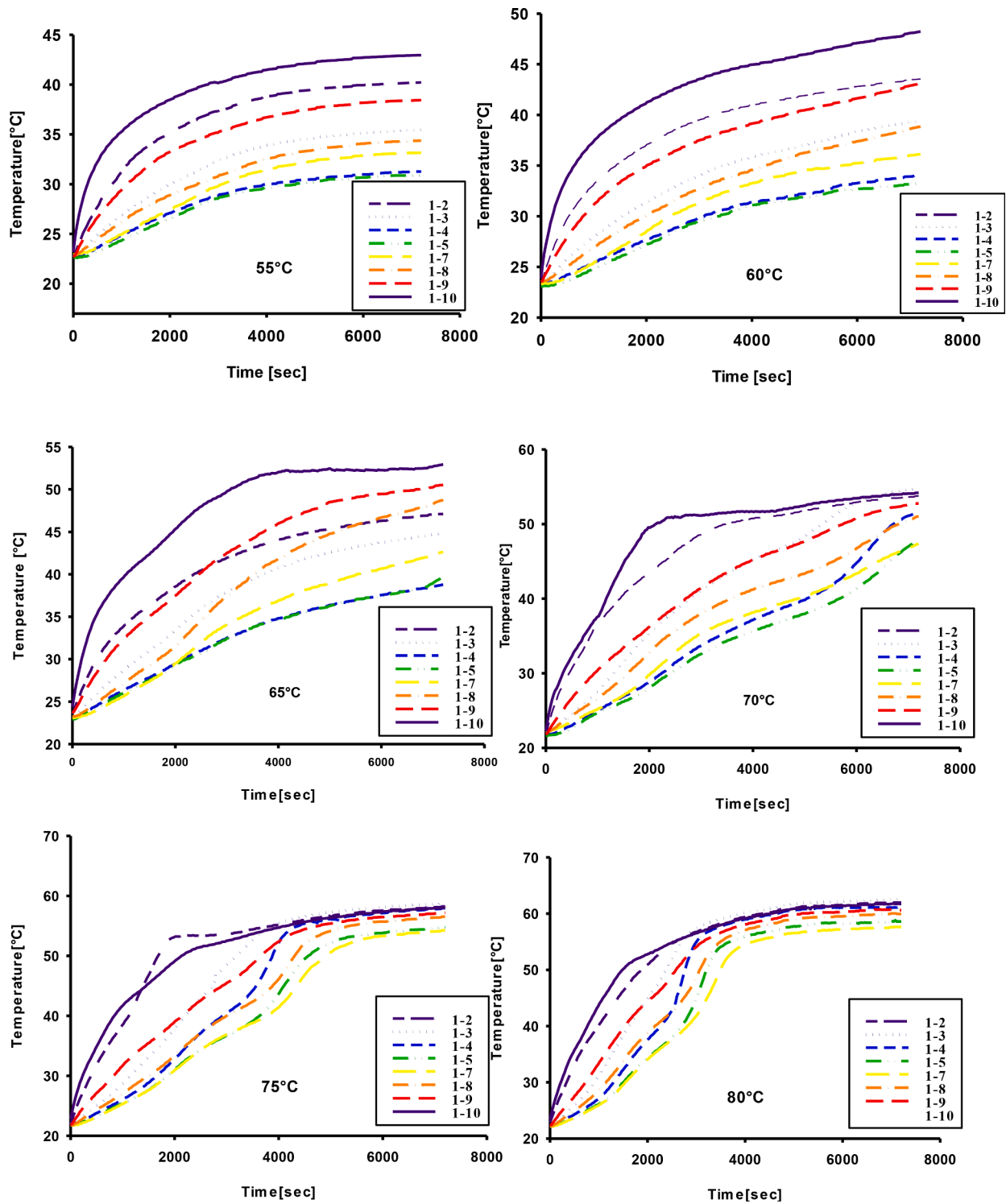


Fig. 6. Temperature distribution of the PCM at constant HTF inlet temperature during melting.

mechanism steps in. Density gradients occur due to the temperature difference. Due to the difference in density, the effect of buoyancy determines in which direction the melting process. This increases the irregular process of the melting in PCM and heat transfer with the effect of natural convection. Liquid PCM float as its density is lower than that of the solid PCM. This explains why the locations close to the T section reached higher temperatures than the B section [15]. In this study, in which the HTF of 70°C was used, the effects of melting started after 1800 sec and complete melting was achieved in 7200 sec when equalize the

1-2,1-3,1-9 and 1-10 location temperatures. With the experiment in, which the inlet temperature of 75°C was used, melting started in 1380 sec at the temperature of 44,67°C. The location temperatures can increase above one other after the melting process. This is caused by the natural convection that affect the progression of the solid-fluid interface in the both radial and axial direction. This can make it hard to make comments in accordance with time and control the melting of the PCM within the system. Melting started at 60°C and firstly at 75°C a completely constant state was achieved in the system where the

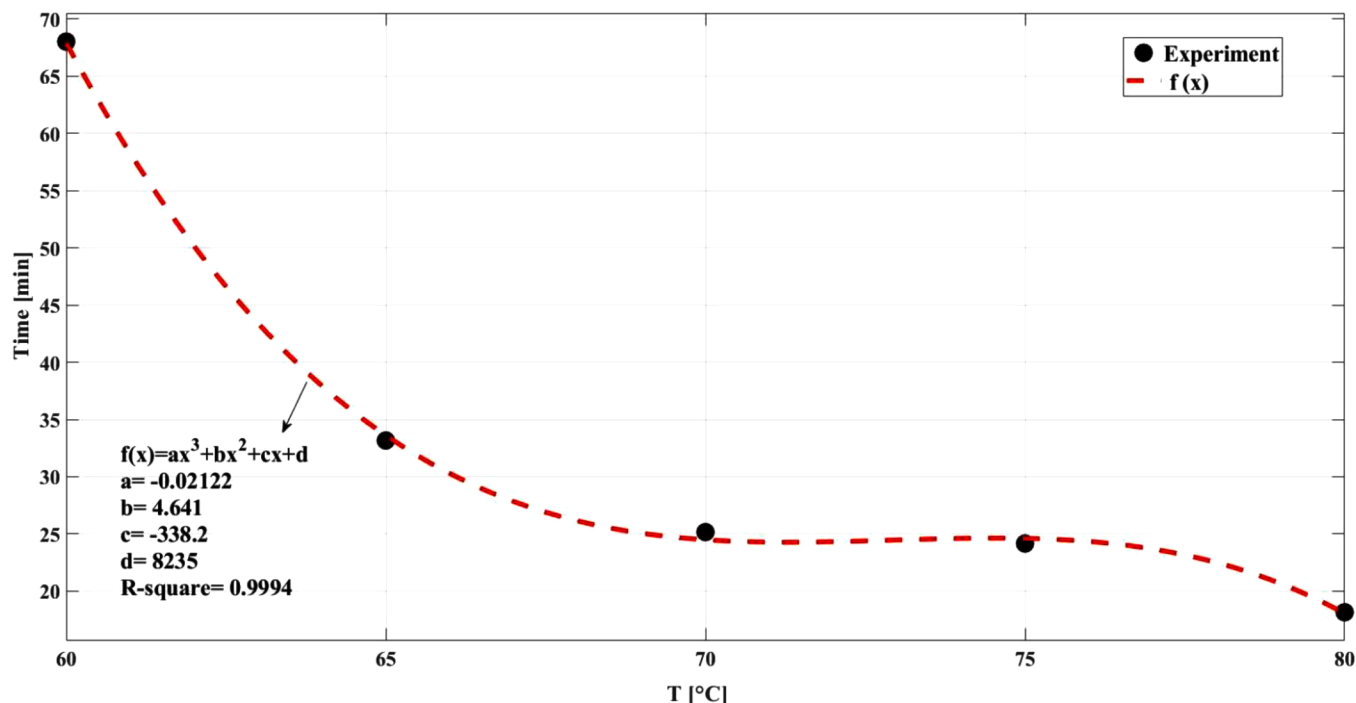


Fig. 7. Melting start time of the PCM at different HTF inlet temperatures.

Table 5
Experimental photographs of the melting for PCM storage at different time.

Inlet Temperature \ Time	40 min	60 min	80 min	100 min	120 min
65 °C	No melting on surface	No melting on surface	No melting on surface		
70 °C	No melting on surface	No melting on surface			
75 °C					
80 °C					

thermocouples were placed. The complete melting state was reached faster at 80°C. Even when the maximum temperature was used, the PCM within the cylindrical enclosure did not melt completely. A long period of time is needed for this.

It is seen from Fig. 7 that the melting of PCM starts at 60°C and continues until the final temperature of 80°C. As the HTF inlet temperature increased, the melting starting time decreased. When the inlet temperature was increased from 60°C to 65°C, the melting starting time decreased by 51.22%, when the inlet temperature was increased from 60°C to 70°C, the melting starting time decreased by 62.99%, when the inlet temperature was increased from 60°C to 75°C, the melting starting time decreased by 64.46% and when the inlet temperature was

increased from 60°C to 80°C, the melting starting time decreased by 73.28%. In these experimental parameters, the melting starting time graph was determined as f(x) function with 99.94% accuracy depending on the HTF inlet temperature.

No melting on the inner surface of plexiglass in the vertical was observed with the constant inlet temperatures of 55°C and 65°C. In addition, with all the other temperatures, solid-liquid interface was begun to be observed after 40 min. As can be seen from Table 4, although melting started around the minichannel after the 34th minute at a constant HTF inlet temperature of 65°C, the solid-liquid interface was observed through the plexiglass between 80-100th min; although melting started after the 25th min at an inlet temperature of 70°C, the

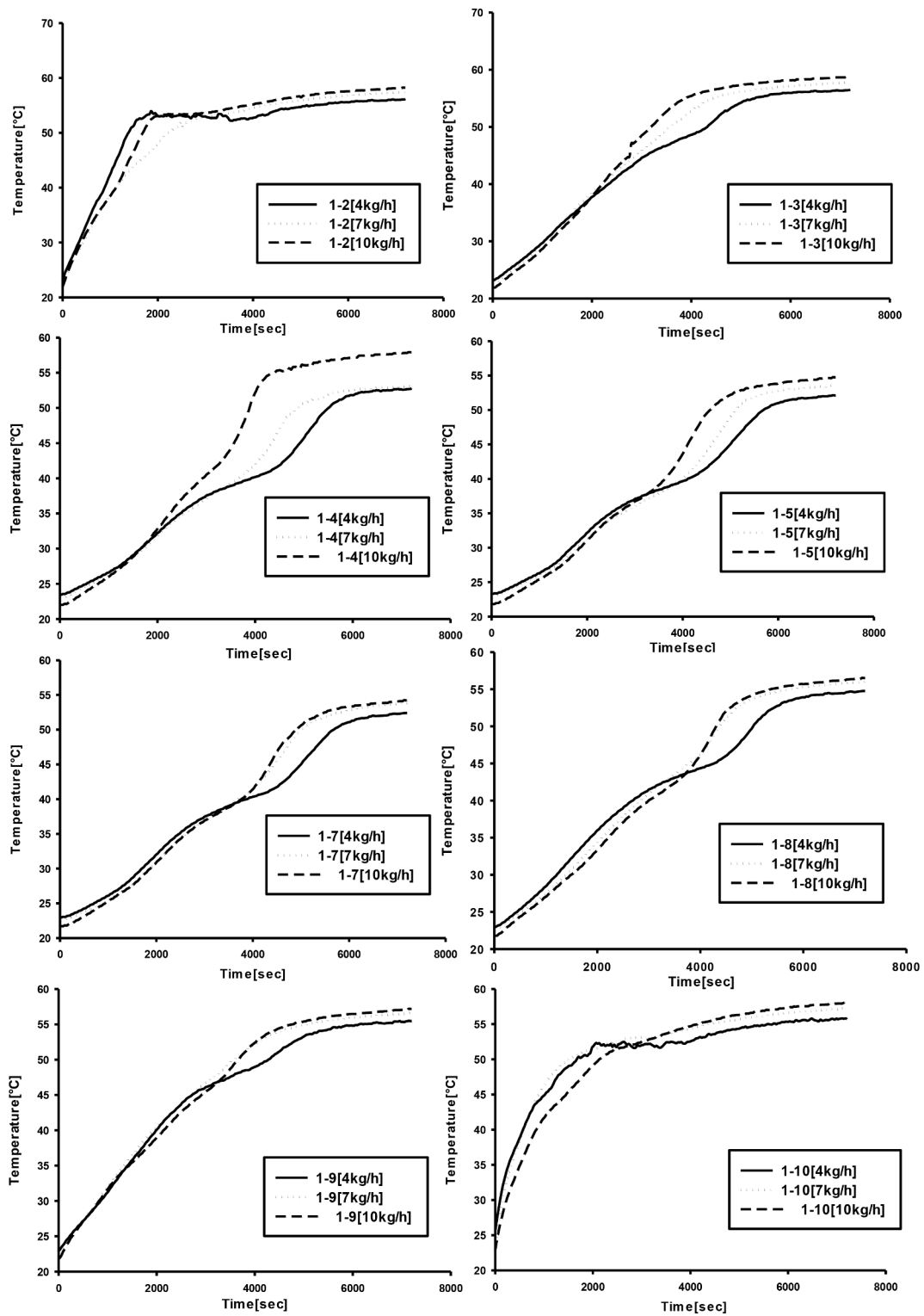


Fig. 8. Effect of HTF flow rate on the PCM.

solid-liquid interface was observed between 60-80th min; although melting started after the 23rd min at an inlet temperature of 75°C, the solid-liquid interface was observed between 40-60th min; although melting started after the 18th min at an inlet temperature of 80°C, the solid-liquid interface was observed 40-60th min. The reason for this was that even though melting had begun around the minichannel, it takes longer to progress to the inner surface of the plexiglass. The density of the liquid PCM decreases as it melts, therefore it goes on top of the solid

PCM. With the maximum temperature of 80°C, although the PCM reached approximately 63°C, there were still some PCM that had not melted completely at lower section (bottom) of the plexiglass enclosure. The aim is how the solid/liquid interface progresses, depending on time and inlet temperature in Table 5.

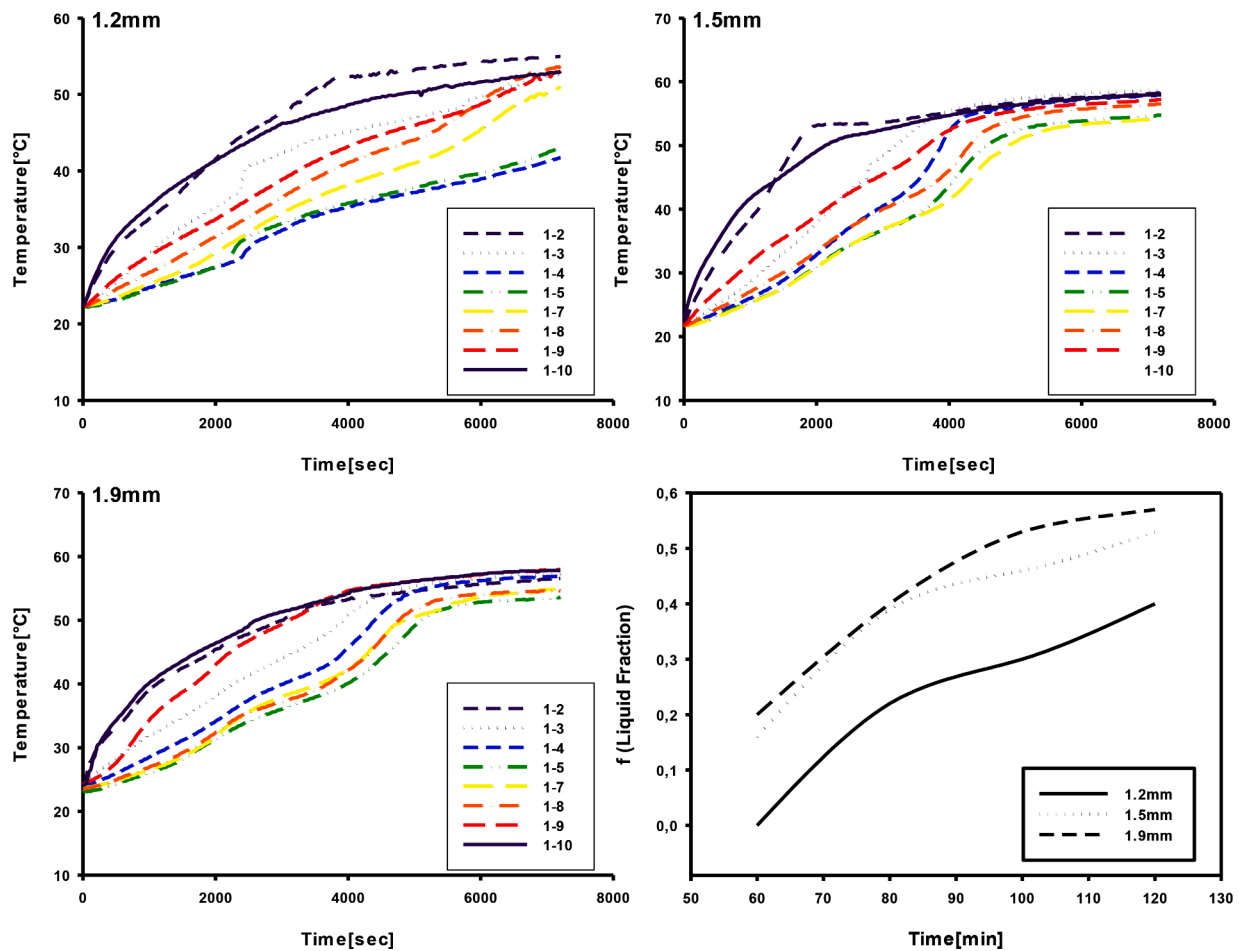


Fig. 9. Effect of minichannel diameter on PCM at 75°C HTF inlet temperature.

3.3. The effect of HTF flow rate on energy storage (charge)

Three different flow rates (4, 7 and 10 kg/h) were studied at constant 1.5mm minichannel diameter and at 75°C, where complete melting was observed firstly. In Fig. 8, the effect of HTF flow rate on TES was studied at locations 3, 6, 9 and 12mm depths in the PCM.

Melting was achieved at all locations at 75°C. Melting time decreased with the increase in the mass flow rate and temperature. However, the effect of mass flow was negligible as it did not cause major changes in the locations. As there is a need for higher pumping power for higher mass flow rates, lower flow rates should be selected for energy storage in terms of energy efficiency.

3.4. The effect of the diameter of the minichannel that HTF passes through on energy storage

For the geometric parameter, 1.21, 1.5 and 1.9mm were used as the three different minichannel diameters. Their behavior in the latent heat thermal storage system was observed. PCM temperature distributions were measured and an experimental comparison between the studied storage units were carried out. The inner diameter changed approximately 0.3 mm, therefore the outer diameter of the enclosure was not changed. This was because no significant changes were going to occur in the amount of PCM, which, in turn, would cause almost no change in the amount of energy storage due to the amount of PCM.

As the amount of fluid in the channel with a constant flow rate increased with the diameter, the heat transfer also increased. As seen in Fig. 9, depending on the increase in the heat transfer rate, the amount of melting, that is, the amount of energy storage, increases as the diameter

of the minichannel increases. Liquid fraction is the ratio of liquid PCM to all PCM. The amount of liquid fraction was a function of the stored energy. As the minichannel surface area increased, it increased the amount of heat transfer. When the diameter was reduced from 1.9 mm to 1.5 mm, the diameter ratio decreased by approximately 21%, while the liquid fraction, that is, the energy storage amount, decreased on average by 10.6%. When the diameter was reduced from 1.5 mm to 1.21 mm, the diameter ratio decreased by approximately 20% and the melting amount decreased by 50.5% on average. The equal diameter percentage increase showed that the increase in the heat transfer decreased logarithmically. As the channel diameter increases, melting increases [36].

3.5. The effect of HTF inlet temperature on the release of the stored energy (discharge)

The high-energy liquid PCM released its thermal energy by transferring it to the HTF passing through the minichannel. It was studied at 10 kg/h constant flow rate, 1.5mm constant minichannel diameter and three different inlet temperature of HTF (8, 15, 23°C).

At the beginning, the PCM was in fluid phase at the temperature range of 60-65°C. Below 50°C, until all the determined points in the PCM reached the solidification temperature, various fluctuations occurred within the PCM and continued until a constant state of matter was reached. The solidification began at the outer surface of the minichannel and went along the diameter to the inside of the PCM. With all the temperatures used, the solid matter state was achieved at all locations in the PCM after 7200 sec. As the melting starts around the minichannel, it is not visible due to the solid PCM barrier on the inner surface of the plexiglass. However, in the solidification process, as the liquid

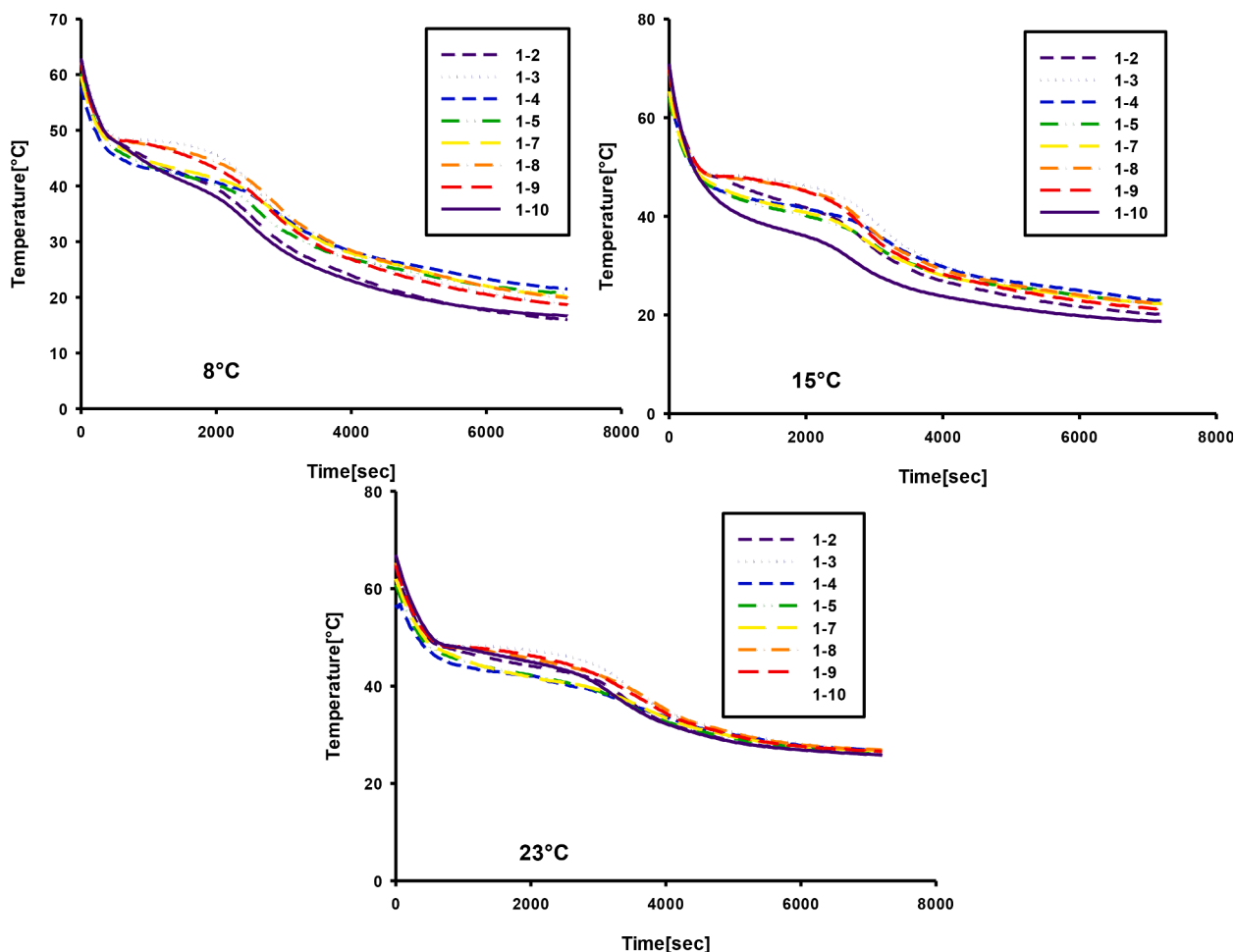


Fig. 10. Temperature distribution of the PCM at constant HTF inlet temperature during solidification.

PCM is transparent, the process is visible. Thus, comments can be made on the progress of melting. Steady state during discharge is defined by the fact that every point of the PCM passed to the solid phase state at radial depths in the measuring plane and sensible heat transfer (conduction) occurred at each point. Here, when the heat transferred to the HTF, its state caused natural convection and phase change within the PCM.

As the temperature difference between PCM and HTF increased in the case of solidification, heat transfer observed to increase. As can be seen from Fig. 10, temperature fluctuations occurred due to natural convection in approximately 0-500 sec for solidification. These fluctuations continued until they reached a steady state in the range of approximately 500-4000 sec. As a result, during discharge as the inlet temperature decreased, the solidification rate increased. This change at average PCM temperature continued until approximately when the room temperature was reached.

As can be seen from in Table 6, solidification first started around the minichannel, but after a specified amount of time, it began to solidify from the bottom to the top of the enclosure contrary to the melting process. This was because the solid PCM sunk to the bottom as it had a higher density. When it reached 8°C at the 620th second, the inner surface of the enclosure had been completely solidified. On the other hand, at 15 and 23°C, the solidification was not completed on the inner walls of the enclosure. This means that as the inlet temperature decreased, the solidification percentage increased. It was observed how the solid-fluid interface advanced physically during the solidification process. In addition, when the solidification image is observed, it can be said that the change occurred throughout the channel during the melting

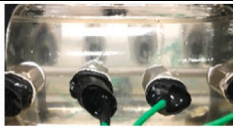
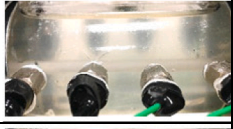
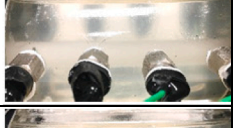
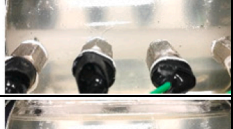
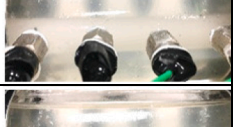
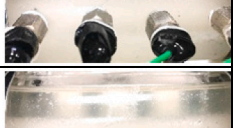
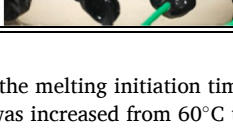
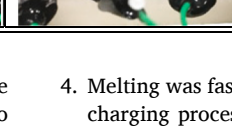
process. Even though the solidification time was a little longer than the melting time, the process happened in the same way [37].

4. Conclusions

In this study, a design different from the literature was used to create an alternative to latent energy storage (LHS) systems by passing minichannels with diameters of 1.21mm, 1.5mm and 1.9mm through a cylindrical enclosure. The thermal performance of the PCM was experimentally investigated by using it between the cylindrical enclosure and the minichannel. Water and RT-50 were used as heat transfer fluid (HTF) and PCM, respectively. The effect of different inlet temperatures of HTF on the thermal performance of the PCM during both charging and discharging has been investigated. In addition, the effect of different flow rates of HTF and different minichannel diameters on the thermal performance of PCM only during charging was studied experimentally. The results are summarized below.

1. The fluid temperature must be at least 10°C above melting temperature of the PCM.
2. Heat transfer decreases and lower temperatures are obtained with distance from the minichannel. Therefore, the maximum temperatures were measured at 12 mm distance from the minichannel. The temperature of positions with the same radial distance can be neglected when sorted from inlet to outlet or outlet to inlet. However, it should be investigated how the reaction will be in a longer test area.

Table 6
Solidification (the energy release) photographs of the PCM at different times.

Temp. Time	8 °C	15 °C	23 °C
0 sec			
20 sec			
80 sec			
140 sec			
200 sec			
260 sec			
320 sec			
380 sec			
440 sec			
500 sec			
560 sec			
620 sec			

3. As the HTF inlet temperature increased, the melting initiation time decreased. When the inlet temperature was increased from 60°C to 65°C, 70°C, 75°C, and 80°C, the melting start time decreased by 51.22%, 62.99%, 64.46%, 73.28%, respectively.

4. Melting was faster, when the inlet temperature increased during the charging process and solidification was faster when the inlet temperature decreased during the discharge process.

5. As the diameter increases in the melting process, heat resistance increases due to the solid PCM and point temperatures decrease in radial distance increase. However, this worked to the opposite effect in the solidification state. Otherwise, the liquid fraction direction progress depends on this resistance.
6. When the minichannel diameter was reduced from 1.9 mm to 1.5 mm and from 1.5 mm to 1.21 mm at 75°C HTF inlet temperature conditions, the liquid fraction which means energy storage percentage was reduced by 10.6% and 50.5%, respectively. It was determined that the effect of the minichannel diameter was important in energy storage. Depending on the increase in the heat transfer rate, the amount of melting, that is, the amount of energy storage, increases as the diameter of the minichannel increases.
7. Melting time decreases as a result of mass flow and temperature increase. However, the effect of the mass flow rate on the melting time at that point is negligible. Since higher mass flow rates require higher pumping power, low flow rate should be chosen for energy storage in terms of energy efficiency.
8. It was concluded that the optimal shell-tube radius ratio could be up to about 25 in the LHTESS systems studied. It is a very important result for engineering systems that use PCM to store energy in heat exchangers.

CRediT authorship contribution statement

Eda Feyza Akyurek: Formal analysis, Supervision, Validation, Writing – original draft, Writing – review & editing. **Mehmet Yoladi:** Conceptualization, Data curation, Investigation, Methodology, Visualization, Writing – original draft, Writing – review & editing.

Declaration of Competing Interest

None.

Acknowledgment

This work was financially supported by Scientific Research Project (SRP) of Erzurum Technical University (Project no: 2019/24).

References

- [1] H.A. Adine, H. El Qarnia, Numerical analysis of the thermal behaviour of a shell-and-tube heat storage unit using phase change materials, *Appl. Math. Model* 33 (2009) 2132–2144, <https://doi.org/10.1016/j.apm.2008.05.016>.
- [2] A.A. Ghoneim, Comparison of theoretical models of phase-change and sensible heat storage for air and water-based solar heating systems, *Sol. Energy* 42 (1989) 209–220, [https://doi.org/10.1016/0038-092X\(89\)90013-3](https://doi.org/10.1016/0038-092X(89)90013-3).
- [3] Z.A. Hammou, M. Lacroix, A hybrid thermal energy storage system for managing simultaneously solar and electric energy, *Energy Convers. Manage.* 47 (2006) 273–288, <https://doi.org/10.1016/j.enconman.2005.01.003>.
- [4] L.F. Cabeza, L. Navarro, A.L. Pisello, L. Olivieri, C. Bartolomé, J. Sánchez, et al., Behaviour of a concrete wall containing micro-encapsulated PCM after a decade of its construction, *Sol. Energy* (2019) 0–1, <https://doi.org/10.1016/j.solener.2019.12.003>.
- [5] A.K. Pandey, M.S. Hossain, V.V. Tyagi, N. Abd Rahim, J.A.L. Selvaraj, A. Sari, Novel approaches and recent developments on potential applications of phase change materials in solar energy, *Renew. Sustain. Energy Rev.* 82 (2018) 281–323, <https://doi.org/10.1016/j.rser.2017.09.043>.
- [6] M. Tao, L. Zhenpeng, Z. Jiaxin, Photovoltaic panel integrated with phase change materials (PV-PCM): technology overview and materials selection, *Renew. Sustain. Energy Rev.* 116 (2019), 109406, <https://doi.org/10.1016/j.rser.2019.109406>.
- [7] U. Stritih, Heat transfer enhancement in latent heat thermal storage system for buildings, *Energy Build.* 35 (2003) 1097–1104, <https://doi.org/10.1016/j.enbuild.2003.07.001>.
- [8] Y. Han, W. Luan, Y. Jiang, X. Zhang, Thermal control of electronics for nuclear robots via phase change materials, *Energy Proc.* 75 (2015) 3301–3306, <https://doi.org/10.1016/j.egypro.2015.07.712>.
- [9] H. Behi, M. Ghanbarpour, M. Behi, Investigation of PCM-assisted heat pipe for electronic cooling, *Appl. Therm. Eng.* 127 (2017) 1132–1142, <https://doi.org/10.1016/j.applthermaleng.2017.08.109>.
- [10] J. Pereira da Cunha, P. Eames, Thermal energy storage for low and medium temperature applications using phase change materials - a review, *Appl. Energy* 177 (2016) 227–238, <https://doi.org/10.1016/j.apenergy.2016.05.097>.
- [11] L. Kalapala, J.K. Devanuri, Influence of operational and design parameters on the performance of a PCM based heat exchanger for thermal energy storage – a review, *J. Energy Storage* 20 (2018) 497–519, <https://doi.org/10.1016/j.est.2018.10.024>.
- [12] I. Al Siyabi, S. Khanna, T. Mallick, S. Sundaram, Multiple phase change material (PCM) configuration for PCM-based heat sinks-an experimental study, *Energies* 11 (2018), <https://doi.org/10.3390/en11071629>.
- [13] M. Mastani Joybari, F. Haghighat, S. Seddegh, Numerical investigation of a triplex tube heat exchanger with phase change material: simultaneous charging and discharging, *Energy Build.* 139 (2017) 426–438, <https://doi.org/10.1016/j.enbuild.2017.01.034>.
- [14] F. Agyenim, N. Hewitt, P. Eames, M. Smyth, A review of materials, heat transfer and phase change problem formulation for latent heat thermal energy storage systems (LHTESS), *Renew. Sustain. Energy Rev.* 14 (2010) 615–628, <https://doi.org/10.1016/j.rser.2009.10.015>.
- [15] M. Akgün, O. Aydin, K. Kaygusuz, Experimental study on melting/solidification characteristics of a paraffin as PCM, *Energy Convers. Manage.* 48 (2007) 669–678, <https://doi.org/10.1016/j.enconman.2006.05.014>.
- [16] A. Rozenfeld, Y. Kozak, T. Rozenfeld, G. Ziskind, Experimental demonstration, modeling and analysis of a novel latent-heat thermal energy storage unit with a helical fin, *Int. J. Heat Mass Transf.* 110 (2017) 692–709, <https://doi.org/10.1016/j.ijheatmasstransfer.2017.03.020>.
- [17] M.A. Kibria, M.R. Anisur, M.H. Mahfuz, R. Saidur, I. Metselaar, Numerical and experimental investigation of heat transfer in a shell and tube thermal energy storage system, *Int. Commun. Heat Mass Transf.* 53 (2014) 71–78, <https://doi.org/10.1016/j.icheatmasstransfer.2014.02.023>.
- [18] A. Sari, K. Kaygusuz, Thermal performance of a eutectic mixture of lauric and stearic acids as PCM encapsulated in the annulus of two concentric pipes, *Sol. Energy* 72 (2002) 493–504, [https://doi.org/10.1016/S0038-092X\(02\)00026-9](https://doi.org/10.1016/S0038-092X(02)00026-9).
- [19] A. Trp, K. Lenic, B. Frankovic, Analysis of the influence of operating conditions and geometric parameters on heat transfer in water-paraffin shell-and-tube latent thermal energy storage unit, *Appl. Therm. Eng.* 26 (2006) 1830–1839, <https://doi.org/10.1016/j.applthermaleng.2006.02.004>.
- [20] S. Seddegh, X. Wang, M.M. Joybari, F. Haghighat, Investigation of the effect of geometric and operating parameters on the thermal behavior of vertical shell-and-tube latent heat energy storage systems, *Energy* 137 (2017) 69–82, <https://doi.org/10.1016/j.energy.2017.07.014>.
- [21] K.A.R. Ismail, M.M. Gonçalves, Thermal performance of a pcm storage unit, *Energy Convers. Manage.* 40 (1999) 115–138, [https://doi.org/10.1016/S0196-8904\(98\)00042-9](https://doi.org/10.1016/S0196-8904(98)00042-9).
- [22] I. Al Siyabi, S. Khanna, T. Mallick, S. Sundaram, An experimental and numerical study on the effect of inclination angle of phase change materials thermal energy storage system, *J. Energy Storage* 23 (2019) 57–68, <https://doi.org/10.1016/j.est.2019.03.010>.
- [23] Z. Li, Z.G. Wu, Analysis of HTFs, PCMs and fins effects on the thermal performance of shell-tube thermal energy storage units, *Sol. Energy* 122 (2015) 382–395, <https://doi.org/10.1016/j.solener.2015.09.019>.
- [24] D. Zhao, G. Tan, Numerical analysis of a shell-and-tube latent heat storage unit with fins for air-conditioning application, *Appl. Energy* 138 (2015) 381–392, <https://doi.org/10.1016/j.apenergy.2014.10.051>.
- [25] Y.Q. Li, Y.L. He, H.J. Song, C. Xu, W.W. Wang, Numerical analysis and parameters optimization of shell-and-tube heat storage unit using three phase change materials, *Renew. Energy* 59 (2013) 92–99, <https://doi.org/10.1016/j.renene.2013.03.022>.
- [26] Y. Pahamli, M.J. Hosseini, A.A. Ranjbar, R. Bahrampoury, Inner pipe downward movement effect on melting of PCM in a double pipe heat exchanger, *Appl. Math. Comput.* 316 (2018) 30–42, <https://doi.org/10.1016/j.amc.2017.07.066>.
- [27] X. Yang, Z. Guo, Y. Liu, L. Jin, Y.L. He, Effect of inclination on the thermal response of composite phase change materials for thermal energy storage, *Appl. Energy* 238 (2019) 22–33, <https://doi.org/10.1016/j.apenergy.2019.01.074>.
- [28] Z.G. Qu, W.Q. Li, W.Q. Tao, Numerical model of the passive thermal management system for high-power lithium ion battery by using porous metal foam saturated with phase change material, *Int. J. Hydrogen Energy* 39 (2014) 3904–3913, <https://doi.org/10.1016/j.ijhydene.2013.12.136>.
- [29] Q. Ren, Z. Wang, T. Lai, J.F. Zhang, Z.G. Qu, Conjugate heat transfer in anisotropic woven metal fiber-phase change material composite, *Appl. Therm. Eng.* 189 (2021), <https://doi.org/10.1016/j.applthermaleng.2021.116618>.
- [30] Z.Y. Jiang, Z.G. Qu, Lithium-ion battery thermal management using heat pipe and phase change material during discharge-charge cycle: a comprehensive numerical study, *Appl. Energy* 242 (2019) 378–392, <https://doi.org/10.1016/j.apenergy.2019.03.043>.
- [31] Q. Ren, P. Guo, J. Zhu, Thermal management of electronic devices using pin-fin based cascade microencapsulated PCM/expanded graphite composite, *Int. J. Heat Mass Transf.* 149 (2020) 1–16, <https://doi.org/10.1016/j.ijheatmasstransfer.2019.119199>.
- [32] Q. Ren, Z. Wang, J. Zhu, Z.G. Qu, Pore-scale heat transfer of heat sink filled with stacked 2D metal fiber-PCM composite, *Int. J. Therm. Sci.* 161 (2021), <https://doi.org/10.1016/j.ijthermalsci.2020.106739>.
- [33] A. Yadav, S. Samir, Experimental and numerical investigation of spatiotemporal characteristics of thermal energy storage system in a rectangular enclosure, *Energy Storage* 21 (2019) 405–417, <https://doi.org/10.1016/j.est.2018.12.005>.
- [34] S.A. Fleischer, *Thermal Energy Storage using Phase Change Materials: Fundamentals and Applications*, 2015, <https://doi.org/10.1007/978-3-319-20922-7>.

- [35] Rubitherm Technologies GmbH. PCM-RT50-Properties n.d. https://www.rubitherm.eu/media/products/datasheets/Techdata_RT50_EN_09102020.PDF (accessed March 25, 2021).
- [36] Q. Li, C. Li, Z. Du, F. Jiang, Y. Ding, A review of performance investigation and enhancement of shell and tube thermal energy storage device containing molten salt based phase change materials for medium and high temperature applications, Appl. Energy 255 (2019), <https://doi.org/10.1016/j.apenergy.2019.113806>.
- [37] M.K. Rathod, J. Banerjee, Experimental investigations on latent heat storage unit using paraffin wax as phase change material, Exp. Heat Transf. 27 (2014) 40–55, <https://doi.org/10.1080/08916152.2012.719065>.